Promotion of palladium-based catalysts on metal monolith for partial oxidation of methane to syngas

Jae-Hong Ryu [a], Kwan-Young Lee [a,*], Hak-Joo Kim [b], Jung-Il Yang [b], Heon Jung [b,**]

[a] Department of Chemical and Biological Engineering, Korea University, 5-1 Anam-dong, Sungbuk-ku, Seoul 136-701, South Korea
[b] Synfuel Research Center, Korea Institute of Energy Research, 71-2 Jang-dong, Yusung-ku, Daejeon 305-343, South Korea

Abstract

Four different modifications of alumina were prepared for use as the support for a Pd catalyst used for the partial oxidation of methane to syngas. The catalysts were washcoated on a metallic monolith in order to determine their activities at high gas flow rates. Compared with the Pd/Al_2O_3 catalyst, enhanced partial oxidation activities were observed with the $Pd/CeO_2/Al_2O_3$, $Pd/CeO_2/BaO/Al_2O_3$ and $Pd/CeO_2/BaO/SrO/Al_2O_3$ catalysts. The palladium particles were better dispersed in the presence of CeO_2 and SrO. Adding BaO, CeO_2 and BaO–CeO_2 to γ-Al_2O_3 prevented the transformation of the alumina phase during the 3-day aging process at 1000 °C, providing the support with some level of thermal stability. The addition of small amounts of SrO to the $CeO_2/BaO/Al_2O_3$ support enhanced the thermal stability of the Pd particles and minimized their sintering. The triply promoted Pd catalyst studied in this work was effective in carrying out partial oxidation at high temperatures, with BaO and CeO_2 promoting the thermal stability of the support, CeO_2 and SrO dispersing the Pd particles and SrO anchoring the Pd particles strongly to the support. The composition of the catalyst which gave both the highest partial oxidation activity and the best thermal stability was $Pd(2)/CeO_2(23)/BaO(11)/SrO(0.8)/Al_2O_3$.
© 2007 Elsevier B.V. All rights reserved.

Keywords: Partial oxidation; Palladium; Ceria; Barium; Strontium

1. Introduction

The partial oxidation (POx) of methane, leading to syngas with a hydrogen to carbon monoxide ratio of about two, can be an ideal reforming process to enhance the utilization of natural gas in the synthesis of methanol and the Fischer–Tropsch reaction [1–6]. The exothermic nature of POx makes the process less energy and capital consumptive than the endothermic steam reforming process. When utilizing a catalyst, the POx process can handle a large volume of the feed gas with only a small amount of the catalyst. The catalytic POx process has other advantages, such as its fast start-up and shut-down capability and good load-following ability. Thus, the catalytic POx process is becoming a preferred technology for the small-scale production of syngas in both stationary and mobile fuel processing systems [7]. The use of monolithic

catalysts can be advantageous for these applications, because it allows the pressure drop to be minimized [8].

In our previous work [9], we reported the application of a palladium-based catalyst washcoated on a metallic monolith to the partial oxidation of methane to syngas. The Pd catalyst showed a CH_4 conversion of more than 90%, even at a high gas hourly space velocity of 108 000 h^{-1}.

The catalysts employed for the production of syngas by the POx process are primarily noble metals catalysts, such as Rh, Ru, Pd or Pt [10–18]. Nickel catalysts have also been studied due to their low cost [19–21]. However, their rapid deactivation by carbon deposition or metal loss at temperatures higher than 700 °C has to be minimized for them to be used for the POx reaction [22]. Noble metal-based POx catalysts are less susceptible to carbon deposition and metal evaporation. However, their thermal stability also needs to be improved for sustained use at the high temperature operations of the POx reaction.

Palladium-based catalysts have been reported to be very effective for methane combustion [23]. Alumina is commonly adopted as a support material to maintain a good dispersion of the active metals. However, palladium catalysts supported on alumina are not stable at the high temperatures associated with

* Corresponding author. Tel.: +82 2 3290 3299; fax: +82 2 926 6102.
** Corresponding author. Tel.: +82 42 860 3663; fax: +82 42 860 3134.
E-mail addresses: kylee@korea.ac.kr (K.-Y. Lee), jungh@kier.re.kr (H. Jung).

methane oxidation reactions. Rare earth and alkaline earth oxides are frequently added to enhance the thermal stability of both the support and the active metal. Low concentrations of barium (Ba) and lanthanum (La) are reported to be very effective in retarding the surface area loss of alumina at high temperatures [24]. Cerium oxide (CeO_2) also provides alumina with thermal stability. However, its stabilizing effect becomes negligible at temperatures higher than 1000 °C under oxidizing conditions [24,25]. Cerium oxide, on the other hand, is known to suppress the deposition of carbon, either by the reaction of carbon with the lattice oxygen [26,27] or by the gasification of carbon with more water that is adsorbed on ceria [28].

Promoters also increase the catalytic activities. Pillai and Sahle-Demessie reported that the addition of strontium was effective in increasing the metal surface area of Pd [29]. The addition of strontium was also found to enhance the basicity of alumina-supported palladium catalysts used for methane combustion [29].

In this work, we studied the effect of Ce, Ba and Sr addition on the activity of alumina-supported Pd catalysts used for the partial oxidation of methane. The addition of these promoters was conducted either individually or in combination. The emphasis was placed on obtaining a highly active catalyst which is thermally stable for sustained operation. The catalysts were prepared in the metal monolith-washcoated form in order to determine their activities at high gas flow rates.

2. Experimental

2.1. Preparation of catalyst

Four alumina-based supports with different promoter materials were prepared, viz. BaO/Al_2O_3, CeO_2/Al_2O_3, $CeO_2/BaO/Al_2O_3$ and $CeO_2/BaO/SrO/Al_2O_3$. The promoted alumina was prepared by the wet impregnation method. Fine particles of γ-Al_2O_3 (Aldrich, 198 m^2/g) were slurried in an aqueous solution of $(C_2H_3O_2)_2$Ba (Aldrich) and/or $(C_2H_3O_2)_3$Ce·xH$_2$O (Aldrich) and/or $(C_2H_3O_2)_2$Sr (Aldrich) at 50 °C for 12 h. The suspension was filtered and dried in air at 120 °C for 3 h. The dried sample was heated to 565 °C at a rate of 2 °C/min and then calcined at that temperature for 3 h. The calcined samples were crushed to fine particles (less than 40 mesh) using a ball-mill. A highly concentrated slurry of fine particles of the promoted alumina and palladium nitrate solution ($Pd(NO_3)_2$) was prepared for the purpose of washcoating the monolith.

The metallic monolith was prepared by winding a combination of a 50 μm-thickness fecralloy plate in a corrugated form (Goodfellow Co.) and a flat fecralloy plate. The monolith had a cell density of about 640 cpi. The monolith was pre-oxidized to enhance the adhesive force between the ceramic-type washcoat material and the metal monolith. Cylindrical metallic monolith catalysts were prepared with a size of 2.2 cm (diameter) × 2 cm (height). The metallic monoliths were dipped into the slurry and dried at room temperature and this process was repeated several times until the desired amount of catalyst was washcoated. The washcoated metallic monoliths were calcined at 900 °C for 8.5 h in air. The amount of the washcoated catalyst was 0.21 g/cm^3 of the monolith. A portion of the slurry was also dried and calcined under the same conditions for the characterization of the catalyst.

2.2. Catalytic reaction

The partial oxidation reaction was carried out in a tubular quartz reactor (inside diameter of 2.22 cm) operated at atmospheric pressure. Fig. 1 shows the experimental apparatus. The reactants, methane and air, were supplied from a cylinder of CH_4 (99.999%) and an air compressor, respectively. The flow rates were controlled by mass flow controllers (Brooks, 5850E).
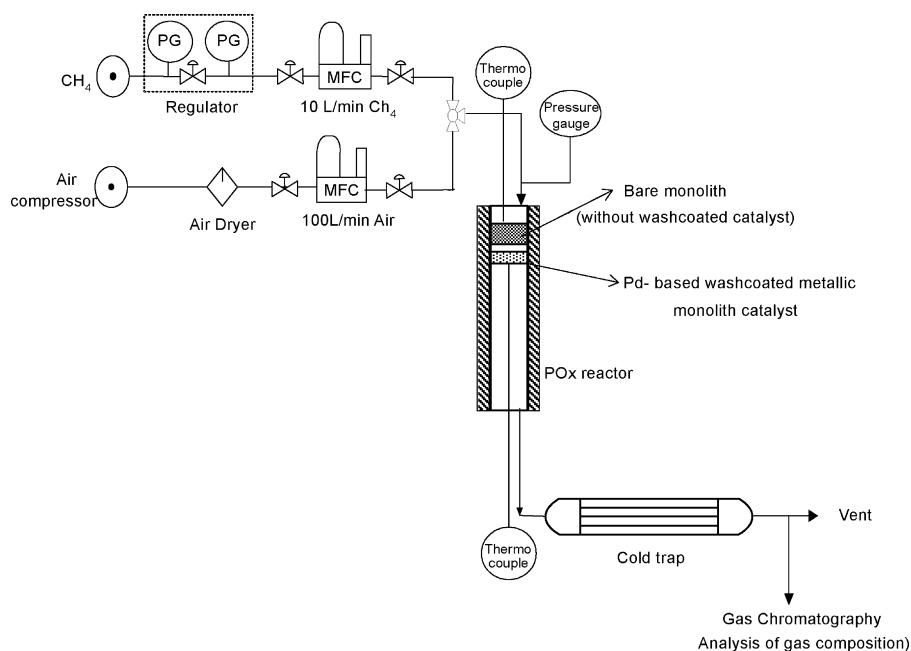

Fig. 1. Schematic of catalytic partial oxidation reaction system.

For the even distribution of the reactant gas, a monolith without the catalyst washcoat was placed in front of the washcoated catalyst. One cylindrical metallic monolith catalyst (2.2 cm diameter and 2 cm height, volume 7.6 cm^3) was used. A thermocouple was placed at the rear end of the monolith catalyst, and its temperature (T_r) was taken as the reaction temperature. Another thermocouple was installed in front of the bare monolith and the temperature read from it (T_f) was used as the reference. During the heating processes, T_r was about the same as T_f. However, once the POx reaction started, T_r became much higher than T_f due to the exothermic heat of the reaction.

A gas mixture of CH_4 and air ($O_2/CH_4 = 0.55$ molar ratio) was passed through the metallic monolith catalyst at a gas hourly space velocity (GHSV) of 100 000 h^{-1}. The GHSV was defined as the ratio of the reactant gas flow rate at 25 °C and 1 atm to the total volume of the catalyst. The compositions of the products were analyzed by a gas chromatograph (HP5890, TCD) equipped with a Porapak Q column (8.2 ft × 1/8 in.). Based on the flow rate and the composition of the product gas, the conversion of CH_4 and the selectivities to H_2 and CO formation were calculated.

2.3. Characterization of the catalysts

The BET surface areas of the support materials, Pd-supported catalysts calcined at 900 °C for 8.5 h and Pd-supported catalysts calcined at 1000 °C for 3 days were measured by an ASAP 2010 instrument (Micromeritics). The powder X-ray diffraction (XRD) patterns of the catalysts were obtained using a Rigaku D/max 2000 ultima plus diffractometer (monochromatic nickel filter, Cu Kα radiation). Inductively coupled plasma-atomic emission spectroscopy (ICP-AES, 138 Ultace, Jobin Yvon) analyses were performed to determine the composition of the catalyst. The morphology and composition of the catalysts washcoated on the metallic monolith were examined by scanning electron microscopy/energy dispersive X-ray analysis (SEM/EDX, HITACHI S-4200).

When palladium was loaded on the support material containing ceria, its metal surface area could not be measured by either hydrogen or CO chemisorption, because both gases adsorb on cerium oxide as well as on palladium [30,31]. Thus, chemisorption analysis was used only for the Pd/alumina catalysts. The Pd surface areas of the other supported catalysts were estimated by measuring the conversion of the cyclohexane dehydrogenation reaction, which is a structure insensitive reaction [32]. The surface area of the Pd particles was reported to be linearly related to the extent of the dehydrogenation [31]. The dehydrogenation reaction was carried out in a packed-bed reactor. The powdered catalyst (10 mg) was dried under N_2 flow (30 ml/min) at 120 °C for 0.5 h. Then, the sample was heated to 460 °C in pure hydrogen flow at a heating rate of 2 °C/min and it was held at this temperature for 1 h. The sample was cooled to 270 °C in hydrogen flow. The reaction mixture was prepared by bubbling hydrogen through a saturator containing cyclohexane (99.999%, Aldrich) at 12 °C ($H_2/C_6H_{12} = 13.2$). The dehydrogenation reaction was carried out at 270 °C with a space velocity (WHSV) of 4.89×10^5 cm^3/g h. Although a high partial pressure of H_2 in the reactant stream retards the dehydrogenation reaction, its presence was necessary to preserve the metallic state of Pd and to inhibit carbon deposition [33,34]. The exit gases were analyzed using an online gas chromatograph (HP5890) equipped with an HP-INNOWAX column. The Pd surface area of each catalyst was then calculated from its conversion of cyclohexane dehydrogenation by comparing with the conversion and the Pd area of Pd/Al$_2$O$_3$ measured by H_2 chemisorption (Micromeritics ASAP 2010).

3. Results

3.1. POx activity of Pd-based catalysts with varying compositions

Table 1 lists the methane conversion of the various Pd-based catalysts washcoated on a metal monolith for the partial oxidation of methane at 700 °C with a gas mixture of O_2/CH_4 ratio of 0.55 and a GHSV of 100 000 h^{-1}. The Pd catalyst on pure α-alumina showed a methane conversion of 80% (case 1). When 21% of BaO was added to alumina, the resulting Pd catalyst showed a slightly lower methane conversion of 78%

Table 1
Conversion and selectivities of methane partial oxidation over Pd catalysts on various promoted alumina supports ($O_2/CH_4 = 0.55$, GHSV = 100 000 h^{-1}, 700 °C)

Case	PdO (%)	CeO$_2$ (%)	BaO (%)	SrO (%)	CH$_4$ conversion (%)	H$_2$ selectivity (%)	CO selectivity (%)
1	2.1	0	0	0	80	76	91
2	2.3	0	21	0	78	60	84
3	2.3	35	0	0	84	76	85
4	2.1	25	10	0	87	85	96
5	2.2	25	10	1	90	83	90
6	2.1	25	5	1	87	83	92
7	2.1	25	10	2	87	84	91
8	2.2	20	10	1	83	81	90
9	2.1	30	10	1	84	85	90
10	2.1	40	10	1	83	80	91
11	1.0	25	11	0.8	88	85	94
12	2.1	25	11	0.8	90	89	92
13	3.0	25	11	0.8	90	87	96
14	4.2	25	11	0.8	90	87	90

Table 2
Surface areas of alumina-based supports obtained after calcination at 565 °C

Supports	CeO$_2$ (wt.%)	BaO (wt.%)	SrO (wt.%)	Al$_2$O$_3$ (wt.%)	BET (m^2/g)
Al$_2$O$_3$	–	–	–	100	155
BaO/Al$_2$O$_3$	–	22	–	78	126
CeO$_2$/Al$_2$O$_3$	38	–	–	62	94
CeO$_2$/BaO/Al$_2$O$_3$	25	10	–	65	81
CeO$_2$/BaO/SrO/Al$_2$O$_3$	25	10	1	64	80

Table 3
Surface areas of Pd-impregnated catalysts

Catalysts	PdO (wt.%)	CeO$_2$ (wt.%)	BaO (wt.%)	SrO (wt.%)	Al$_2$O$_3$ (wt.%)	BET (m^2/g) calcined at 900 °C for 8.5 h	BET (m^2/g) calcined at 1000 °C for 3 days
Al$_2$O$_3$	–	–	–	–	100	78	–
PdO/Al$_2$O$_3$	2.1	–	–	–	97.9	79	9
PdO/BaO/Al$_2$O$_3$	2.3	–	21	–	76.7	94	25
PdO/CeO$_2$/Al$_2$O$_3$	2.3	35	–	–	66.7	76	26
PdO/CeO$_2$/BaO/Al$_2$O$_3$	2.1	26	10	–	61.9	72	19
PdO/CeO$_2$/BaO/SrO/Al$_2$O$_3$	2.0	23	11	0.8	63.2	70	25

Concentration of promoters and Pd measured by ICP.

(case 2). On the other hand, the addition of 35% of CeO$_2$ to alumina increased the methane conversion (case 3).

It should be pointed out that the supports were calcined at 565 °C and the Pd-impregnated catalysts were calcined at 900 °C. The surface areas of several representative support materials and Pd catalysts are listed in Tables 2 and 3, respectively. The calcination at 900 °C for 8.5 h resulted in a decrease in the surface area of the γ-alumina-supported Pd catalyst from 155 m^2/g to 79 m^2/g, a reduction of 49%. However, the BaO-added Pd/alumina showed a reduction in its surface area from 126 m^2/g to 94 m^2/g (25% reduction) after calcination. The addition of 35% CeO$_2$ to alumina led to only a 19% reduction of the surface area after its calcination at 900 °C.

The dispersion of the Pd particles calculated from the conversion data of the cyclohexane dehydrogenation reaction is listed in Table 4. The dispersion of the Pd particles in the case of the Pd/Al$_2$O$_3$ catalyst was 4.3%, suggesting the occurrence of severe sintering of the Pd particles and/or blockage of the pores during its calcination at 900 °C for 8.5 h. The BaO-added Pd catalyst had a higher Pd dispersion, probably due to the stabilized support. Baria–alumina is known to possess good thermal stability, due to the formation of a layered barium hexa-aluminate structure at high temperatures that prevents the

Table 4
The dispersion of the Pd particles calculated from the conversion of the cyclohexane dehydrogenation reaction

Catalyst	As-prepared catalyst (calcination at 900 °C)	Aged catalyst (calcination at 1000 °C for 3 days)
PdO/Al$_2$O$_3$	4.3	1.7
PdO/BaO/Al$_2$O$_3$	14.7	6.1
PdO/CeO$_2$/Al$_2$O$_3$	28.6	–
PdO/CeO$_2$/BaO/Al$_2$O$_3$	29.4	–
PdO/CeO$_2$/BaO/SrO/Al$_2$O$_3$	33.8	23.7

formation of α-alumina, thus suppressing the decrease of the surface area [35,36]. However, its lower methane POx conversion as compared to that of the alumina-supported Pd catalyst suggests that there might exist a negative effect of the excessive BaO doping on the Pd particles.

Contrary to the common belief that the role of ceria as a thermal stabilizer is limited, the addition of 35% CeO$_2$ to alumina preserved both the support structure and the Pd particles during calcination at 900 °C. The Pd dispersion of the ceria-added catalyst was 28.6%, which resulted in a higher methane conversion for the POx reaction. Ceria is known both to disperse and to stabilize metal particles, due to the strong metal support interaction (SMSI) [36,37]. The SMSI caused by ceria might contribute to the higher dispersion of the Pd particles, which eventually led to a high methane conversion of the ceria-added Pd catalyst for the POx reaction.

When both ceria and BaO were added to alumina, the total surface area was reduced by 11% during calcination and the dispersion of the Pd particles was 29.4%. The methane conversion over this catalyst was 87% (case 4). In the case of the combined addition of ceria and BaO to alumina, BaO is known to stabilize the alumina phase while ceria stabilizes the metallic dispersion [36]. The higher methane conversion of the Pd/BaO/CeO$_2$/Al$_2$O$_3$ catalyst (case 4) than that of the Pd/CeO$_2$/Al$_2$O$_3$ catalyst (case 3) might come from the fact that the case 4 catalyst contained less ceria (25%) than the case 3 catalyst (35%). A similar trend of higher methane combustion activities was observed with a Pd/BaO/CeO$_2$/Al$_2$O$_3$ catalyst having a lower ceria content [38]. It was suggested that the stabilization of the Pd particles was achieved only when the amount of ceria on the support was in an optimum value [38].

The Pd catalyst supported on the 1% SrO-added BaO/CeO$_2$/Al$_2$O$_3$ support showed 90% methane conversion in the POx reaction at 700 °C (case 5). The Pd catalyst with a similar SrO content (0.8%) had a high Pd dispersion of 33.8% (Table 4) and

the methane POx conversion over this catalyst was also 90% (case 12). Strontium was found to be an effective promoter for enhancing the Pd metal area, the percentage dispersion of Pd and the hydrogenation activity of the supported Pd catalysts [29]. The promotional effect of SrO on the supported Pd catalysts is probably caused by both a change in the net charge density at the metal and an enhancement in the metal dispersion [29]. When the SrO addition was increased to 2% (Sr/Pd = 1), the methane conversion decreased to 87% (case 7). Pillai and Sahle-Demessie also observed that the maximum promotion of SrO was achieved when the Sr/Pd ratio was 0.5 [29]. In our case, the highest methane POx conversion was obtained from the Pd catalysts with a Sr/Pd ratio between 0.4 and 0.5.

Reducing the amount of BaO added from 10% to 5% resulted in a slightly less active catalyst (case 6), suggesting that the optimum BaO content was about 10%. Changing the ceria content from 20% to 40% (case 8, case 5, case 9 and case 10) revealed that the optimum ceria content was about 25%. Our result is consistent with the finding of Liotta and Deganello [38], who reported that the promotional effect of ceria was only observed up to a certain amount and that the effect disappeared at a higher ceria loading.

The palladium loading on the optimized Al_2O_3–CeO_2–BaO–SrO support (cases 11–14) was varied from 1% to 4%. Increasing the Pd loading above 2% did not result in any improvement in the partial oxidation activity. Thus, the optimum composition of the Pd-based catalyst for the partial oxidation of methane was close to $Pd(2)/CeO_2(23)/BaO(11)/SrO(0.8)/Al_2O_3$.

3.2. POx activity of aged catalysts

Fig. 2 shows the CH_4 conversion of the POx reaction over the five different Pd catalysts on the metallic monolith as a function of the temperature with a reaction gas mixture having an O_2/CH_4 ratio of 0.55 and a GHSV of 100 000 h^{-1}. The gas temperature was measured at the exit of the catalyst. As was discussed in the previous section, Fig. 2 shows that the POx activity was in the order $Pd/BaO/Al_2O_3 < Pd/Al_2O_3 < Pd/CeO_2/Al_2O_3 < Pd/BaO/CeO_2/Al_2O_3 < Pd/BaO/CeO_2/SrO/Al_2O_3$. This trend of activity was maintained over the whole temperature range between 700 °C and 900 °C.

To simulate accelerated aging, the above five catalysts were subjected to an air environment at 1000 °C for 3 days. Fig. 3 shows the CH_4 conversion of the POx reaction over the aged Pd catalysts on the metallic monolith as a function of the temperature. The surface areas of the resulting catalysts are listed in Table 3. The POx activity of the Pd/Al_2O_3 catalyst was significantly reduced by the aging treatment and the resulting methane conversion was about 40%. The significant reduction of the activity of the aged Pd/Al_2O_3 catalyst was due to its lower thermal stability, which resulted in a decrease of both the total surface area from 79 m^2/g to 9 m^2/g and a decrease in the Pd dispersion from 4.3% to 1.7%.

The addition of BaO, CeO_2 and BaO–CeO_2 to alumina preserved the support structure to a certain extent, resulting in surface areas in the range between 19 m^2/g and 26 m^2/g after
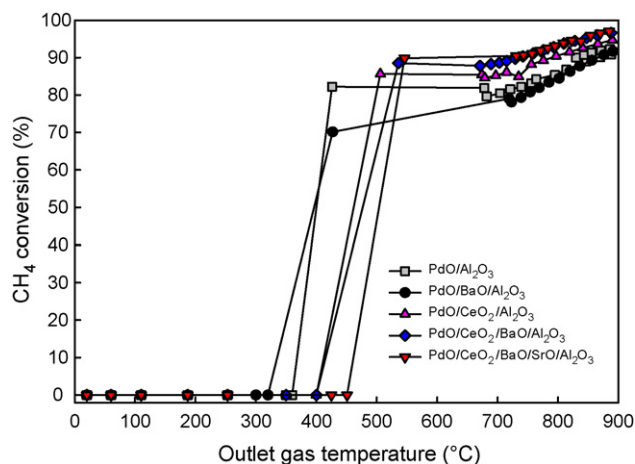

Fig. 2. Temperature-programmed partial oxidation of methane over selected Pd catalysts impregnated on promoted alumina (3.51 L/min CH_4, 9.19 L/min air and catalyst volume = 7.6 cm^3).

aging. Their methane conversion at 850 °C was approximately 60%, which is about 30% lower than their conversion without the aging treatment. In the case of $Pd/BaO/Al_2O_3$, the Pd dispersion was reduced from 14.7% to 6.1% after aging.

The POx activity of the $Pd/BaO/CeO_2/SrO/Al_2O_3$ catalyst suffered to the least extent after the severe aging treatment (Fig. 3). This result is surprising when considering the fact that the $Pd/BaO/CeO_2/SrO/Al_2O_3$ catalyst also lost a large portion of its total surface area during the aging process (70 → 25 m^2/g). However, the aging reduced the Pd dispersion to a less extent from 33.8% to 23.7%. These results provide a clear indication that SrO played a significant role in stabilizing the Pd particles at high temperatures.

4. Discussion

The XRD patterns of the Pd catalysts supported on γ-Al_2O_3, CeO_2/Al_2O_3, BaO/Al_2O_3, $CeO_2/BaO/Al_2O_3$ and $CeO_2/BaO/SrO/Al_2O_3$ prepared by calcination at 900 °C are shown in Fig. 4. The palladium in the as-prepared catalysts is in an oxide
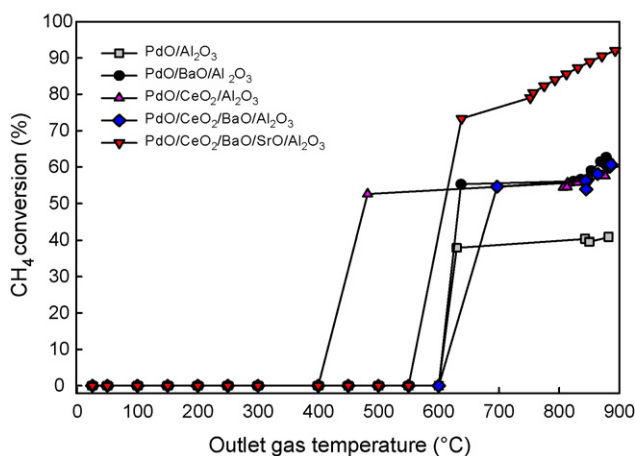

Fig. 3. Temperature-programmed partial oxidation of methane over aged Pd catalysts (3.51 L/min CH_4, 9.19 L/min air, catalyst volume = 7.6 cm^3).
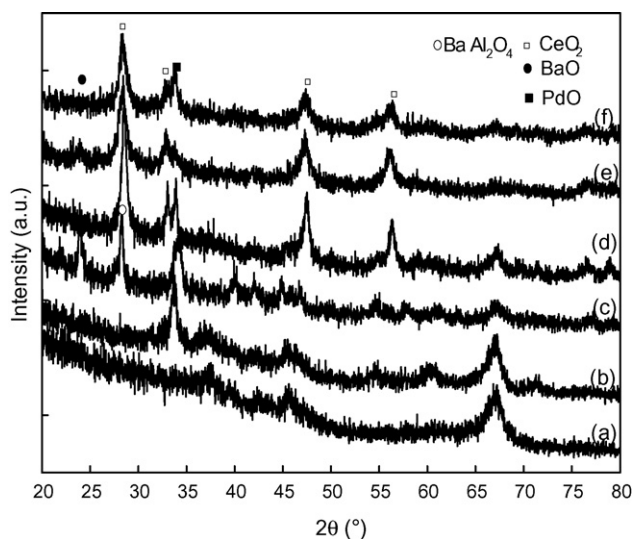
Fig. 4. XRD patterns of the Pd catalysts calcined at 900 °C: (a) γ-Al$_2$O$_3$, (b) PdO/Al$_2$O$_3$, (c) PdO/BaO/Al$_2$O$_3$, (d) PdO/CeO$_2$/Al$_2$O$_3$, (e) PdO/CeO$_2$/BaO/Al$_2$O$_3$ and (f) PdO/CeO$_2$/BaO/SrO/Al$_2$O$_3$.

form (tetragonal PdO at $2\theta = 33.89°$). The alumina phases (γ-Al$_2$O$_3$) remained intact in all of the catalysts during the catalyst preparation at 900 °C. In the case of the Pd/BaO/Al$_2$O$_3$ catalyst, BaO phase as well as the BaAl$_2$O$_4$ phase were observed. Crystalline CeO$_2$ phase was evident in all of the ceria-containing catalysts.

After the aging treatment at 1000 °C for 3 days, the γ-Al$_2$O$_3$ support of the Pd/Al$_2$O$_3$ catalyst was transformed into α-alumina (Fig. 5). The transformation of the alumina phase resulted in a significant loss of the total surface area (Table 3) and the Pd particles also suffered from sintering during the transformation (Table 4). The agglomeration of the Pd particles can be observed from the TEM image shown in Fig. 6.

The addition of BaO, CeO$_2$ and BaO–CeO$_2$ to γ-Al$_2$O$_3$ prevented the transformation of the alumina phase during the
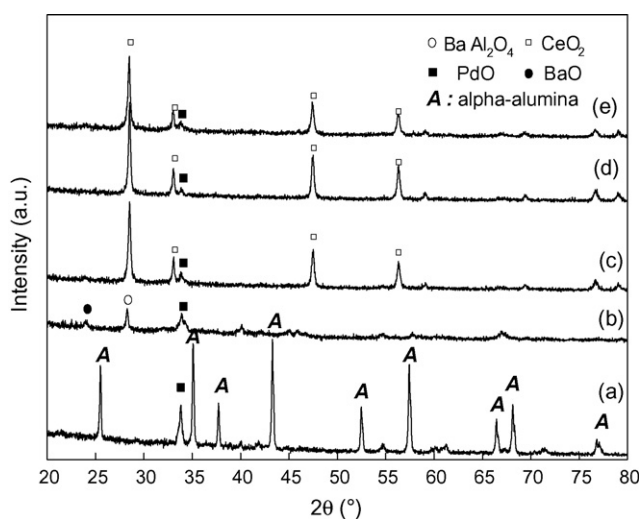

Fig. 5. XRD patterns of the aged catalysts calcined at 1000 °C for 3 days: (a) PdO/Al$_2$O$_3$, (b) PdO/BaO/Al$_2$O$_3$, (c) PdO/CeO$_2$/Al$_2$O$_3$, (d) PdO/CeO$_2$/BaO/Al$_2$O$_3$ and (e) PdO/CeO$_2$/BaO/SrO/Al$_2$O$_3$.
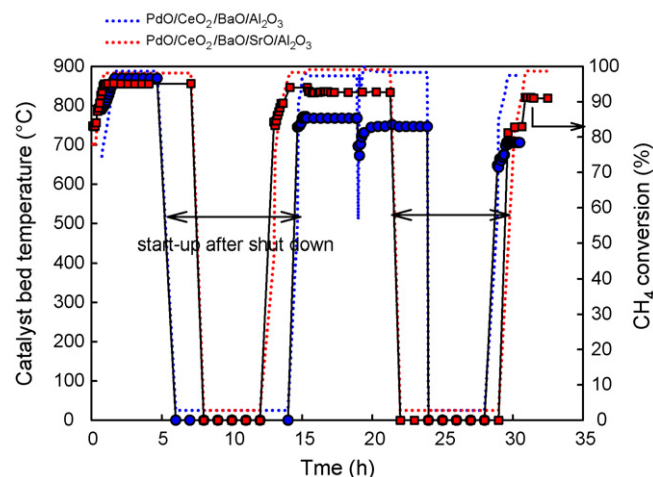

Fig. 6. Change in methane partial oxidation activity of promoted Pd catalysts during cyclic on-off operation (O$_2$/CH$_4$ = 0.55, GHSV = 100 000 h^{-1}, ●: PdO/CeO$_2$/BaO/Al$_2$O$_3$, ■: PdO/CeO$_2$/BaO/SrO/Al$_2$O$_3$).

aging process (Fig. 5), preserving the support structure and leading to surface areas in the range between 19 m^2/g and 26 m^2/g. Although the XRD spectra of the aged catalysts show the presence of more crystalline CeO$_2$ phases, the Pd particles were still well dispersed on the promoted supports, as evidenced by the broader XRD peaks.

The optimum Pd-based catalyst (Pd(2)/CeO$_2$(23)/BaO(11)/SrO(0.8)/Al$_2$O$_3$) had both high activity for the partial oxidation of methane and high-thermal stability. These characteristics come from the combined effects of the three promoters. BaO provided the alumina support with thermal stability as well as basicity [39]. Ceria also provided the support with thermal stability [25,40,41].

The PdO phase was reduced to Pd in the reducing environment of the partial oxidation reaction, as was evidenced by our XPS analysis of the spent Pd catalyst. Ceria also enhanced the activity of the Pd catalysts by increasing the reducibility of the PdO particles [41,42]. Yue et al. showed that the reducibility of supported palladium catalysts was an important factor influencing their catalytic properties [43,44]. Ceria can prevent coke deposition, which enables more stable operation of the POx reaction [26,27,45].

SrO was crucial in generating and maintaining well-dispersed Pd particles during the high temperature operation. Strontium was reported to be an efficient promoter for enhancing the Pd metal area and the hydrogenation activity of supported Pd catalysts [29]. In another perovskite catalytic system, strontium doping stabilized Ru by preventing agglomerization and evaporation loss at high temperatures [46]. The enhanced thermal stability afforded by SrO promotion was also observed in the case of an Ni/SrO–SiO$_2$ catalyst used in CO$_2$ reforming [47]. In this catalytic system, the SMSI induced by SrO played a dominant role in maintaining the bound state of the Ni particles on the support. The same interaction might also exist in our triply promoted Pd catalyst, where the strong interaction caused by SrO prevented the agglomerization of the Pd particles during the high temperature reaction.
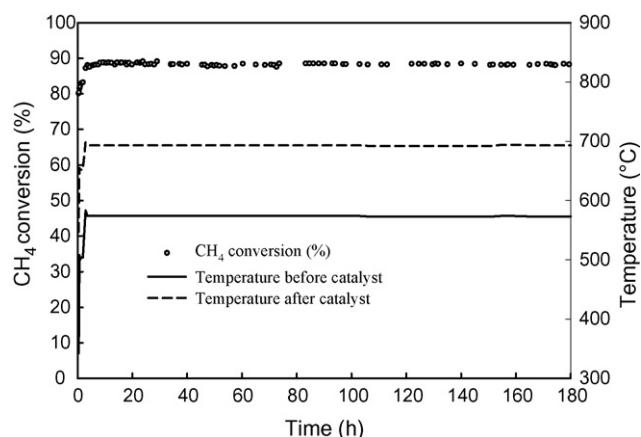
Fig. 7. Long-term methane partial oxidation activity of PdO/CeO$_2$/BaO/SrO/Al$_2$O$_3$ at 693 °C (O$_2$/CH$_4$ = 0.55, GHSV = 100 000 h^{-1}).

To confirm the effect of SrO addition on the catalytic stability, the cyclic on/off operation of the methane POx reaction was carried out at 900 °C over both the SrO-added Pd catalyst and the Pd catalyst without SrO addition. As shown in Fig. 6, both the Pd/CeO$_2$/BaO/SrO/Al$_2$O$_3$ catalyst and the Pd/CeO$_2$/BaO/Al$_2$O$_3$ catalyst exhibited high initial activities. However, the Pd/CeO$_2$/BaO/Al$_2$O$_3$ catalyst gradually lost its partial oxidation activity after the repeated shut-downs and start-ups. On the other hand, the SrO-added Pd catalyst showed lower rate of deactivation, and it retained a methane conversion of more than 90% after 2 cycles of on/off operation.

At the lower temperatures the stability of the triply promoted Pd catalyst was more evident. Fig. 7 shows the long-term stability test of a triply promoted Pd catalyst at the lower temperature of 693 °C. As can be seen, the catalyst was stable with no loss of activity for 180 h.

5. Conclusions

The effect of Ce, Ba and Sr addition on the activity of the alumina-supported Pd catalyst used for the partial oxidation of methane was studied, in order to obtain a highly active catalyst which has sufficient thermal stability for sustained operation at high temperatures. The addition of BaO resulted in a more stable support. The addition of ceria improved both the thermal stability of the support and the activity of the Pd catalyst. The combined addition of ceria and BaO also improved the thermal stability of the support and enhanced the activity of the Pd catalyst. The addition of BaO, CeO$_2$ and BaO–CeO$_2$ to γ-Al$_2$O$_3$ prevented the transformation of alumina phase during the 3-day aging process at 1000 °C. The addition of small amounts of SrO to the CeO$_2$/BaO/Al$_2$O$_3$ support increased the dispersion of the Pd particles, which led to higher partial oxidation activity. More importantly, SrO enhanced the thermal stability of the Pd particles, so that the deactivation due to the sintering of the Pd particles is minimized. The triply promoted Pd catalyst studied in this work was effective in carrying out partial oxidation at high temperatures and its optimum composition for both the high activity and the stability was Pd(2)/CeO$_2$(23)/BaO(11)/SrO(0.8)/Al$_2$O$_3$.

References

[1] M.E. Dry, J.R. Anderson, M. Boudart, Catalysis: Science and Technology, vol. 1, Springer Verlag, New York, 1981.
[2] C.K. Rofer-de-Poorter, Chem. Rev. 81 (1981) 447.
[3] R.B. Anderson, The Fischer Tropsch Synthesis, Academic Press, New York, 1984.
[4] R.H. Jones, A.T. Ashcroft, D. Waller, Catal. Lett. 8 (1991) 169.
[5] P.D.F. Vernon, M.L.H. Green, A.K. Cheetham, Catal. Lett. 6 (1990) 181.
[6] M.A. Goula, A.A. Lemonidou, W. Grunert, M. Baerns, Catal. Today 32 (1996) 149.
[7] C. Song, Catal. Today 77 (2002) 17.
[8] S. Irandoust, B. Andersson, Catal. Rev. Sci. Eng. 30 (1998) 341.
[9] H. Jung, W.L. Yoon, H. Lee, J.S. Park, J.S. Shin, H. La, J.D. Lee, J. Power Sources 72 (2004) 408.
[10] A.T. Ashcroft, A.K. Cheethan, J.S. Foord, M.L.H. Green, C.P. Grey, A.J. Murrel, P.D.F. Vernon, Nature 344 (1990) 319.
[11] A.K. Bhattacharya, J.A. Breach, S. Chand, D.K. Chorai, A. Hartidge, J. Keary, K.K. Mallick, Appl. Catal. A 80 (1992) L1.
[12] Y. Boucouvalas, Z.L. Zhang, X.E. Verykios, Catal. Lett. 40 (1996) 189.
[13] D.A. Hickman, E.A. Haupfear, L.D. Schmidt, Catal. Lett. 17 (1993) 223.
[14] V.R. Choudhary, A.S. Mamman, S.D. Sansare, Angew. Chem. Int. Ed. Eng. 31 (1992) 1189, Appl. Catal. 90 (1992) L1.
[15] V.R. Choudhary, A.M. Rajput, B. Prabhaker, J. Catal. 139 (1993) 326.
[16] Y.L. Chu, S.B. Li, J.F. Gu, Y.L. Yang, Appl. Catal. A 134 (1996) 67.
[17] D. Dissanayake, M.P. Rosynek, K.C.C. Kharas, J.H. Lunsford, J. Catal. 132 (1991) 117.
[18] D.A. Hickman, L.D. Schmidt, J. Catal. 138 (1992) 267.
[19] V.R. Choudhary, V.H. Rane, A.M. Rajput, Catal. Lett. 22 (1993) 289.
[20] Y.H. Hu, M.E. Ruckenstein, J. Catal. 158 (1996) 260.
[21] T. Zhu, M. Flytzani-Stephanopoulos, Appl. Catal. A 208 (2001) 403.
[22] L. Pino, V. Recupero, S. Beninati, A.K. Shukla, M.S. Hegde, P. Bera, Appl. Catal. A 225 (2002) 63.
[23] K. Narui, K. Furuta, H. Yata, A. Nishida, Y. Kohtoku, T. Matsuzaki, Catal. Today 45 (1998) 173.
[24] J.S. Church, N.W. Cant, D.L. Trimm, Appl. Catal. A: Gen. 101 (1993) 105.
[25] A. Piras, A. Trovarelli, G. Dolcetti, Appl. Catal. B: Environ. 28 (2000) L77.
[26] L.V. Mattos, E.R. de Oliveira, P.D. Resende, F.B. Noronha, F.B. Passos, Catal. Today 77 (2002) 245.
[27] K. Otsuka, Y. Wang, E. Sunada, I. Yamanaka, J. Catal. 175 (1998) 152.
[28] Y.H. Wang, J.C. Zhang, Fuel 84 (2005) 1926.
[29] U.R. Pillai, E. Sahle-Demessie, Appl. Catal. A 281 (2005) 31.
[30] F.B. Passos, E.R. de Olivira, L.V. Mattos, F.B. Noronha, Catal. Today 101 (2005) 23.
[31] P.P. Silva, F.A. Silva, H.P. Souza, A.G. Lobo, L.V. Mattos, F.B. Noronha, C.E. Hori, Catal. Today 101 (2005) 31.
[32] F.B. Passos, R. Frety, M. Schmal, Catal. Lett. 29 (1994) 109.
[33] R. Frety, P.N. da Silva, M. Guenin, Catal. Lett. 3 (1989) 9.
[34] E. Rogemond, N. Essayem, R. Frety, V. Perrichon, M. Primet, F. Mathis, J. Catal. 166 (1997) 229.
[35] M. Machida, K. Educhi, H. Arai, J. Catal. 103 (1987) 385.
[36] L.F. Liotta, G. Deganello, D. Sannino, M.C. Gaudino, P. Ciambelli, S. Gialanella, Appl. Catal. A 229 (2002) 217.
[37] S. Bernal, J.J. Calvino, M.A. Caqui, J.M. Catica, C. Larese, J.A. Perez Omil, J.M. Pintado, Catal. Today 50 (1999) 175.
[38] L.F. Liotta, G. Deganello, J. Mol. Catal. A: Chemical 204 (2003) 763.
[39] B. Djuricic, S. Pickering, D. Mcgarry, J. Mater. Sci. 34 (1999) 2685.
[40] P.O. Thevenin, A. Alcalde, L.J. Pettersson, S.G. Järås, J.L.G. Fierro, J. Catal. 215 (2003) 78.
[41] B. Yue, R. Zhou, Y. Wang, X. Zheng, Appl. Catal. 295 (2005) 31.
[42] R. Monterio, F. Noronha, L. Dieguez, M. Schmal, Appl. Catal. A: Gen. 131 (1995) 89.
[43] B. Yue, R. Zhou, Y. Wang, X. Han, X. Zheng, Appl. Surf. Sci. 246 (2005) 36.
[44] B. Yue, R. Zhou, Y. Wang, X. Zheng, J. Mol. Catal. A 238 (2005) 241.
[45] D.L. Trimm, Catal. Today 49 (1999) 3.
[46] A.L. Sauvet, J. Fouletier, F. Gaillard, M. Primet, J. Catal. 209 (2002) 25.
[47] Q. Jing, H. Lou, J. Fei, Z. Hou, X. Zheng, Int. J. Hydrogen Energy 29 (2004) 1245.